TISSUE ENGINEERING: Part A
Volume 19, Numbers 15 and 16, 2013

DOI: 10.1089/ten.tea.2012.0567

Biomimetic Engineering of Nanofibrous Gelatin Scaffolds with Noncollagenous Proteins for Enhanced Bone Regeneration

Yao Sun, DDS, PhD,[1,2] Yong Jiang, DDS, PhD,[1,3] Qilin Liu, DDS, PhD,[1,4] Tian Gao, BS,[1] Jian Q. Feng, MD, PhD,[1] Paul Dechow, PhD,[1] Rena N. D'Souza, DDS, PhD,[1] Chunlin Qin, DDS, PhD,[1] and Xiaohua Liu, PhD[1]

Biomimetic approaches are widely used in scaffolding designs to enhance tissue regeneration. In this study, we integrated noncollagenous proteins (NCPs) from bone extracellular matrix (ECM) with three-dimensional nanofibrous gelatin (NF-Gelatin) scaffolds to form an artificial matrix (NF-Gelatin-NCPs) mimicking both the nanostructured architecture and chemical composition of natural bone ECM. Through a chemical coupling process, the NCPs were evenly distributed over all the surfaces (inner and outer) of the NF-gelatin-NCPs. The *in vitro* study showed that the number of osteoblasts (MC3T3-E1) on the NF-Gelatin-NCPs was significantly higher than that on the NF-Gelatin after being cultured for 14 days. Both the alkaline phosphatase (ALP) activity and the expression of osteogenic genes (*OPN, BSP, DMP1, CON,* and *Runx2*) were significantly higher in the NF-Gelatin-NCPs than in the NF-Gelatin at 3 weeks. Von Kossa staining, backscattered scanning electron microscopy, and microcomputed tomography all revealed a higher amount of mineral deposition in the NF-Gelatin-NCPs than in the NF-Gelatin after *in vitro* culturing for 3 weeks. The *in vivo* calvarial defect study indicated that the NF-Gelatin-NCPs recruited more host cells to the defect and regenerated a higher amount of bone than the controls after implantation for 6 weeks. Immunohistochemical staining also showed high-level mineralization of the bone matrix in the NF-Gelatin-NCPs. Taken together, both the *in vitro* and *in vivo* results confirmed that the incorporation of NCPs onto the surfaces of the NF-Gelatin scaffold significantly enhanced osteogenesis and mineralization. Biomimetic engineering of the surfaces of the NF-Gelatin scaffold with NCPs, therefore, is a promising strategy to enhance bone regeneration.

Introduction

The biomimetic approach is one of the most important strategies of scaffolding design for tissue regeneration.[1–5] Several technologies, such as electrospun and molecular self-assembly, have been developed to prepare synthetic nanofibrous scaffolds that mimic the nano-structured architecture of natural extracellular matrix (ECM).[6–10] Due to the simplicity and capability of use for a variety of natural and synthetic biomaterials, electrospun is the most widely used method to fabricate nanofibrous matrices.[7,8] However, this technique typically forms two-dimensional (2D) sheets, and is difficult to make three-dimensional (3D) scaffolds with a well-defined pore size and geometry, which is considered to be crucial for facilitating cell distribution and guiding tissue regeneration.[11,12] Molecular self-assembly is a useful tool to fabricate supramolecular architectures, and many biomolecules (e.g., peptides and proteins) have been reported to self-assemble into hydrogels with a nanofibrous structure.[13–15] Although molecular self-assembly is a fairly new method for the formation of nano-structured scaffolds, the mechanical property of the self-assembled hydrogels is very low, which limits its applications to tissue regeneration. Using a thermally induced phase separation combined with particle leaching technique, we recently prepared 3D nanofibrous gelatin (NF-Gelatin) scaffolds with high surface areas, high porosities, well-interconnected macropores, and nanofibrous pore wall structures.[16] The NF-Gelatin scaffolds mimic both the chemical composition and physical architecture of natural collagen (the most abundant organic component of the ECM in many tissues) and have been demonstrated to be a promising scaffold for bone tissue regeneration.[17]

[1]Biomedical Sciences Department, The Center for Craniofacial Research and Diagnosis, Texas A&M University Baylor College of Dentistry, Dallas, Texas.
[2]School of Stomatology, Tongji University, Shanghai, China.
[3]School of Stomatology, Fourth Military Medical University, Xi'an, China.
[4]School of Stomatology, Jilin University, Changchun, China.

In natural bone ECM, there are noncollagenous proteins (NCPs), which include, but are not limited to, bone sialoprotein (BSP), osteopontin (OPN), dentin sialophosphoprotein (DSPP), matrix extracellular phosphoglycoprotein (MEPE) and dentin matrix protein 1 (DMP1). Recent studies have indicated that these NCPs play a significant role in osteogenesis and mineralization.[18–21] For example, DMP1 is highly expressed in osteocytes and, when deleted in mice, causes defective osteocyte maturation, leading to pathological changes in bone mineralization.[22] In a subcutaneous transplantation mice model, DMP1 has been shown to induce the generation of dental pulp-like tissue when combined with dental pulp stem cells and a collagen scaffold.[23] However, to date, little is known about the effects of these NCPs on bone tissue regeneration.

In this work, we developed a surface-engineering technique to incorporate the NCPs onto the nanofibrous surfaces of the 3D gelatin scaffolds. The NCP-modified NF-Gelatin scaffold mimics both the nano-fibrous architecture and chemical compositions of the natural ECM of bone. We hypothesize that the novel biomimetic scaffold will promote bone tissue formation and mineralization, resulting in the generation of bone with a better quality than the NF-Gelatin scaffolds alone. For the *in vitro* study, we select MC3T3-E1 preosteoblasts because MC3T3-E1 is the most widely accepted cell line for the study of osteoblasts adhesion, proliferation, differentiation, and biomineralization in 3D scaffolds. Furthermore, *in vivo* experiments were performed to evaluate this surface-engineered biomimetic scaffold.

Materials and Methods

Materials

Gelatin (type B, from bovine skin, ~225 Bloom) was purchased from Sigma Chemical Company. N-hydroxysuccinimide (97%) (NHS) and (2-(N-morpholino) ethanesulfonic acid) hydrate (MES) were purchased from Aldrich Chemical. 1-Ethyl-3-(3-dimethylaminopropyl) carbodiimide hydrochloride (EDC) was purchased from Pierce Biotechnology. Ethanol, hexane, cyclohexane, and 1,4-dioxane were purchased from Fisher Scientific.

Extraction of NCPs

NCPs were extracted from the long bones of 6-week-old rats (Sprague Dawley, Harlan) as previously described.[24] Briefly, the long bones of the rats were dissected and frozen in liquid nitrogen to be crushed into small pieces, which were further ground into powders. The non–mineral-associated proteins and cells inside the bone powder were removed using 200 mL guanidine hydrochloride (Gdm-HCl, 4 M) in a sodium acetate (50 mM) solution. Next, a 4M Gdm-HCl/0.5 M EDTA solution (200 mL) with a proteinase inhibitor cocktail (50 mM 6-amino-n-caproic acid, 25 mM benzamidine HCl, 0.5 mM N-ethylmaleimide, and 0.3 mM PMSF) was added to release the proteins in the mineral matrix for 2 days. The extract was clarified by centrifugation at 10,000 *g* for 30 min. The protein solution was dialyzed using 10-kDa dialysis cassettes (Pierce) in 4°C cold water for 3 days. The dialysized solution was freeze-dried to obtain the NCPs. The complete compositions of the NCPs are still unclear to date. However, it is generally accepted that the NCP mixture mainly includes DMP1, DSPP, BSP, OPN, osteonectin, and several bone matrix proteoglycans.[19,25] The proteins are predominantly from 10 to 300 kDa.[19] All staining results showed that OPN, DMP1, and BSP are rich in this mixture (Supplementary Fig. S1; Supplementary Data are available online at www.liebertpub.com/tea). The presence of OPN, DMP1, and BSP was confirmed by western blot analyses using specific antibodies.[24]

Preparation of fluorescein isothiocyanate-labeled NCPs

The NCPs (50 mg) and fluorescein isothiocyanate (FITC; 10 mg) were dissolved in borate buffer (10 mL, pH 9.5) at 37°C. The FITC solution was then mixed with the NCP solution and incubated in darkness at 37°C for 24 h. The reacted mixture was extensively dialyzed against distilled water. The water was changed every 12 h for 4 days until no free FITC was detected in the dialyzing water. The FITC-conjugated NCP solution was freeze-dried and stored in darkness at 4°C for further use.

Surface modification of NF-Gelatin scaffolds with NCPs

NF-Gelatin scaffolds were fabricated as previously described.[16] Briefly, paraffin spheres (0.40 g, 250–420 μm) were pretreated in Teflon molds at 37°C for 40 min. Gelatin (2.0 g) was dissolved in water (10 mL) and ethanol (10 mL) solvent mixture at 45°C, and this solution was cast onto the paraffin sphere assembly. The gelatin solution in the paraffin assembly was then phase-separated at −76°C for at least 4 h. After leaching the paraffin and solvent exchange, the scaffolds were freeze-dried and cut to the required size (5.0 mm diameter and 1.5 mm thickness). To couple the NCPs with NF-Gelatin scaffolds, the NCPs (5 mg) were first dissolved in 5 mL MES buffer (pH 5.3, 0.05 M). NF-Gelatin scaffolds (50 mg) were added to the NCP solution, and they were crosslinked using EDC and NHS at 4°C for 24 h. To maintain the nanostructure and the swelling of the gelatin scaffold, acetone/water (90/10, v/v) solvent mixtures were used during the crosslinking process. Glycine was added to block the unreacted groups, and the scaffolds were washed 3 times with distilled water at 37°C. The scaffolds were freeze-dried for 3 days and then stored in a desiccator for later use. The unreacted NCPs in the solution were concentrated and measured using a MicroBCA protein assay (Pierce). The amount of NCPs coupling with the NF-Gelatin scaffold, therefore, was obtained by subtracting the unreacted NCPs from the total NCPs in the solution. To visualize the distribution of NPCs inside the NF-Gelatin scaffolds, FITC-labeled NPCs were used for the crosslinking reaction. As a control, NF-Gelatin scaffolds were prepared under the same conditions except that no NCPs were added during the crosslinking process.

Mechanical test

The compressive modulus of scaffolds was measured using a mechanical tester (TestResources). Scaffolds were incubated in water for 24 h before the test. Before the test, the scaffolds were taken out and the excess water on the surface of the scaffolds was gently blotted with a filter paper. The compressive modulus was measured as reported previously.[16,17] All the samples were circular discs (16 mm in diameter and

2 mm in thickness). The specimens were compressed at a crosshead speed of 0.5 mm/min and the stress vs. strain curve was recorded. The modulus was calculated as the slope of the linear portion of the stress–strain curve. The averages and standard deviations (SDs) were reported ($n = 6$).

Cell culture and seeding on scaffolds

The MC3T3-E1 cells were cultured in a supplemented α-minimum essential medium (MEM) with 10% fetal calf serum (Gibco), including several reagents (100 U/mL glutamine, 100 U/mL penicillin, 100 U/mL streptomycin, 50 μg/mL ascorbic acid, 10 mM β-glycerophosphate) in a humidified incubator at 37°C with 5% CO_2. During cell culture, most of the MC3T3-E1 exhibited a spindle-like shape with extended cytoplasmic processes. The cell morphology of the MC3T3-E1 remained stable for at least 10 passages, and passages 4–5 were used for this study. Gelatin scaffolds were sterilized with 70% ethanol for 2 h. The scaffolds were washed three times (30 min each) with phosphate-buffered saline (PBS; Invitrogen) to remove the residual ethanol. After that, the scaffolds were washed twice with α-MEM containing 10% fetal bovine serum. The cells (5×10^5) were seeded on each scaffold in a seeding tray. After 0.5 h, the cell–scaffold constructs were removed from the seeding trays and transferred into 12-well tissue culture plates containing 2 mL of complete medium in each well. The constructs were cultured on the orbital shaker at 80 rpm in a humidified incubator at 37°C with 5% CO_2. The medium was changed every other day. At 7 and 14 days after cell seeding, the amount of total DNA on the scaffolds was measured.

DNA assay

The amount of cells on the scaffolds was determined using a DNA assay kit (BioTek USA). The cell–scaffold constructs were homogenized in 1 mL of DNA assay buffer (Sigma) using a homogenizer. One milliliter of cell lysis buffer was added, and the samples were incubated at 37°C for 1 h. The cell lysis was spun down at 5000 *g* for 5 min. The total DNA was quantified using a fluorescence assay with Hoechst 33258 dye according to the manufacturer's instructions.

Scanning electron microscopy observation

Scanning electron microscopy (SEM) observation was performed as described earlier.[26] For resin-casted examination, the samples were dissected and fixed in 2.5% glutaraldehyde in 0.1 M sodium cacodylate buffer containing 0.05% tannic acid. The tissue specimens were dehydrated in ascending concentrations of ethanol (from 70% to 100%), embedded in methyl methacrylate, and then surface polished using 1 μm and 0.3 μm Alpha Micropolish Alumina II (Buehler) on a soft-cloth rotating wheel. The bone surface was acid etched with 37% phosphoric acid for 2–10 s, followed by 5% sodium hypochlorite for 5 min. The samples were coated with gold and palladium and examined using an FEI/Philips XL30 Field-Emission Environmental SEM at 10 kV as described previously.[26]

Alkaline phosphatase activity

Alkaline phosphatase (ALP) activity was detected using a TRACP & ALP Kit (Takara) according to the manufacturer's protocol. The scaffolding construct was washed with PBS, and the cells on the scaffold were homogenized in 1 mL lysis buffer supplied with the kit. The lyses were centrifuged at 10,000 *g* and 4°C for 15 min. Supernatant was collected, and the absorbance was measured at 405 nm. The amount of ALP in the cells was normalized against total protein content.

Real-time reverse transcription–polymerase chain reaction

The total mRNA from the cells was extracted using Trizol (Invitrogen). First-strand cDNA was synthesized using a QuantiTect Rev Transcription Kit (Qiagen). The sequences of the specific primer sets were the following: ALP (sense 5′-ACGTGGCTAAGAATGTCATC-3′; antisense 5′-CTGGTAGGCGATGTCCTTA-3′); DMP1 (sense 5′-TGGGGATTATCCTGTGCTCT-3′; antisense 5′-TACTTC TGGGGTCACTGTCG-3′); osteocalcin (sense 5′-CATGA GAGCCCTCACA-3′; antisense 5′-AGAGCGACACCCTA GAC-3′); OPN (sense, 5′-GGTGATAGCTTGGCTTATGG ACTG-3′; antisense, 5′-GCTCTTCATGTGAGAGGTGAGG TC-3′); and glyceraldehyde-3-phosphate dehydrogenase (GAPDH; sense 5′-AGCCGCATCTTCTTTTGCGTC-3′; antisense 5′-TCATATTTGGCAGGTTTTTCT-3′). The mean values from triplicate analyses were compared. The quantitative reverse transcription–polymerase chain reaction (qRT-PCR) was performed using Brilliant SYBR Green QPCR Master Mix (Applied Biosystems) and the Bio-rad Real-Time PCR Detection System (Bio-Rad). The PCR conditions were initial denaturation at 95°C for 10 min, followed by 45 cycles of 95°C for 30 s, 60°C for 1 min, and 72°C for 30 s. The levels of genes in the experimental group were expressed as fold changes relative to the level in the control group.

X-ray radiography and microcomputed tomography

The *in vitro* cultured scaffolds were analyzed by X-ray radiography (Faxitron) and a μ-CT35 imaging system (Scanco Medical). The microcomputed tomography (μ-CT) analysis is a high-resolution scan (3.5 μm slice increment) of the scaffold (5 mm diameter, 1.5 mm thick). The data acquired from the high-resolution scans were used for quantitative analyses. The quantitative CT parameter bone volume (BV), total volume (TV), and bone volume to total volume ratio (BV/TV) were obtained and analyzed using the Scanco software.

Histology analysis

After 3 weeks of culturing, the scaffolds were rinsed with PBS and fixed with 4% paraformaldehyde. To prepare the undemineralized sections, the specimens were embedded in methylmethacrylate and cut in 10-μm-thick sections using a Leica rotary microtome (Leica). Using a von Kossa Kit (Polysciences), the undemineralized sections were stained by von Kossa staining to compare the quantity of calcified bone matrix according to the manual.

Surgical procedures

A total of 30 male rats (6 weeks, Sprague Dawley; Harlan) were used for this study. The rats were evenly divided into three groups: (a) NF-Gelatin-NCPs; (b) NF-Gelatin; and (c) empty control. All animals were anesthetized by intramuscular injection of xylazine/ketamine and submitted to trichotomy of the frontoparietal region of the head, vigorous

disinfection with iodophor alcohol, and isolation of the surgical area. An incision (1.5 cm) was made in the skin of the skull with a surgical knife in order to expose the cranial bone surface of the region. The periosteum was stripped. Using a surgical trephine measuring 5 mm in diameter, a central perforation was created in the skull bone under abundant and continuous irrigation with physiological saline. The defects were filled with NF-Gelatin-NCPs and NF-Gelatin scaffolds, respectively. The stripped periosteum was placed in position and closed with sutures. Six weeks after surgery, the animals were euthanized and the skulls were harvested for μ-CT, histological, and immunohistochemistry examination.

Radiographic procedures

The animals were sacrificed by injection of an overdose of the anesthetics. The skullcap of each animal with overlying skin was removed and immediately placed in 4% PFA in phosphate buffer (pH = 7.4). After fixation for 1 week, the specimens were measured by the μ-CT imaging system mentioned above.

Histological procedures

The specimens were demineralized in 10% EDTA for 3 weeks in a 4°C refrigerator. The specimens were sequentially washed under water, dehydrated in ethanol, cleared in xylene, and embedded in paraffin. The specimens were cut in the laterolateral direction into alternating 5-μm-thick sections and stained with hematoxylin–eosin for histological examination. For immunohistochemistry staining, rehydrated sections were pretreated with hyloronadase solution for 60 min and incubated with primary antibody for 1 h. For the detection of DMP1, anti-DMP1-C-8G10.3 antibodies[27] were used at a dilution of 1:800. To identify BSP and OPN, antibodies were used at a dilution of 1:500, and to distinguish BSP, anti-BSP-10D9.2 monoclonal Ab[24] was used at dilution of 1:400. To detect OPN, the anti-OPN monoclonal Ab (Santa Cruz Biotechnology) was used at a dilution of 1:400. Since osterix (OSX) is a zinc finger-containing transcriptional factor that is essential for osteoblast differentiation and bone formation, we also included it in the immunohistochemical staining study. For the detection of OSX, the anti-sp7/ OSX rabbit polyclonal Ab (Abcam) was used at a dilution of 1:400. All immunohistochemistry experiments were performed with an ABC kit and DAB kit (Vector Laboratories, Inc.) according to the manufacturer's instructions.

Statistical analysis

All data are presented as mean ± SD. To test the significance of the observed differences between the two groups, an unpaired Student's *t*-test was applied. A value of $p < 0.05$ was considered to be statistically significant.

Results

Preparation and characterization of NF-Gelatin-NCPs scaffolds

NF-Gelatin scaffolds were fabricated by combining a thermally induced phase separation and porogen leaching technique.[16] The NF-Gelatin scaffold had a high interconnected macroporous structure (Fig. 1a) and nanofibrous

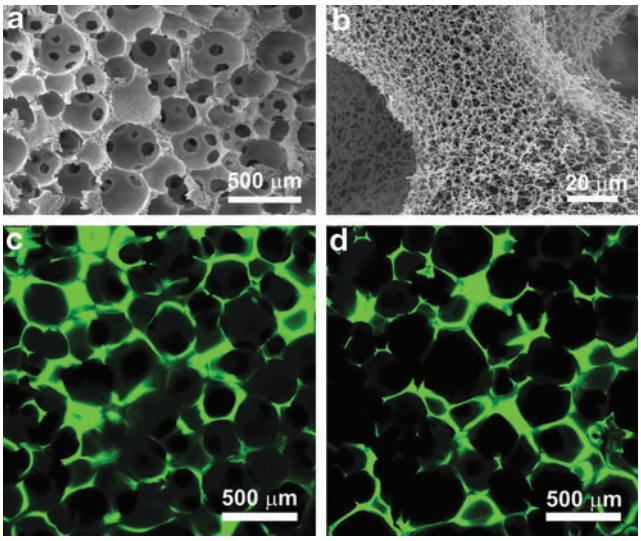

FIG. 1. Characterization of noncollagenous protein (NCP)-modified nanofibrous gelatin (NF-Gelatin) scaffolds. **(a)** Scanning electron microscopy (SEM) image of a three-dimensional NF-Gelatin scaffold, overview; **(b)** high magnification of the NF-Gelatin scaffold, showing the nanofibrous architecture of its pore walls; **(c, d)** confocal image of the NF-Gelatin scaffold after coupling with fluorescein isothiocyanate-labeled NCPs. Image **(c)** was taken from the outermost edge of the scaffold, and image **(d)** was taken from the inner surface of the scaffold (~400 μm from the outside surface). Both **(c)** and **(d)** show that the NCPs were distributed evenly over the surfaces of the entire scaffold. Color images available online at www.liebertpub.com/tea

architecture of pore walls (Fig. 1b). The diameter of the NF-Gelatin nanofibers ranged from 50 to 500 nm, which is the same as that of natural collagen fiber bundles. Using a chemical coupling process, the NCPs were successfully conjugated onto the surfaces of the NF-Gelatin scaffolds, as indicated by the spectrum of ATR-FTIR (Supplementary Fig. S2) and the confocal images (Figs. 1c, d). The confocal images of the NF-Gelatin-NCP scaffolds further showed that the NCPs (labeled with FITC) were distributed evenly over the entire (both outer and inner) scaffold surfaces. Under our experimental conditions, the amount of NCPs on the surfaces of the NF-Gelatin-NCPs was a 26 ± 8 μg/mg scaffold. A higher amount of NCPs could be deposited onto the surface of the NF-Gelatin by increasing the concentration of NCPs during the coupling reaction (data not shown). In wet state, both the NF-Gelatin and NF-Gelatin-NCP scaffolds retained their original sizes of the dry state and had similar compressive modulus (26.1 ± 4.7 kPa [NF-Gelatin] *vs.* 25.4 ± 5.2 kPa [NF-Gelatin-NCPs]), indicating that the surface coupling process did not affect the mechanical property of the NF-Gelatin-NCPs scaffolds (Fig. 2).

Cell adhesion, proliferation, and differentiation on NF-Gelatin/NF-Gelatin-NCPs scaffolds

More MC3T3-E1 osteoblasts attached on the NF-Gelatin-NCPs than on the NF-Gelatin scaffold 1 day after cell seeding ($p < 0.05$) (Fig. 3). At day 14, the DNA amount on the NF-Gelatin-NCPs (25.9 ± 4.3 μg/scaffold) was more than 54.2% higher than on the NF-Gelatin (16.8 ± 4.8 μg/scaffold),

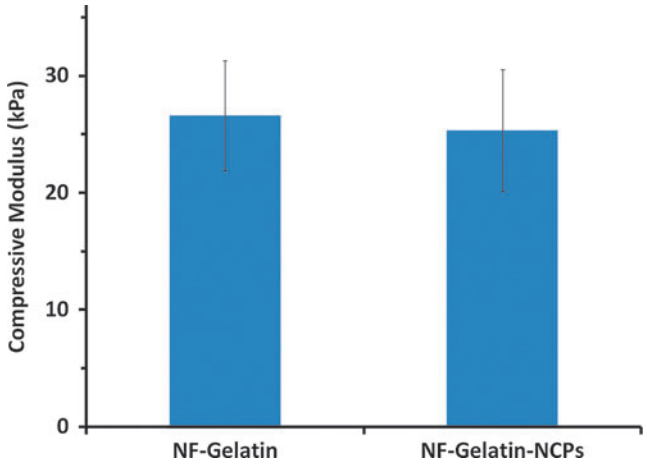

FIG. 2. The compressive modulus of the NF-Gelatin and NF-Gelatin-NCPs scaffolds in wet state. The scaffolds were prepared from a 10.0% (wt/v) gelatin solution in an ethanol/water mixture (ethanol/water = 50/50), and had a macropore size of 250–420 μm and a porosity of about 97.0%. Color images available online at www.liebertpub.com/tea

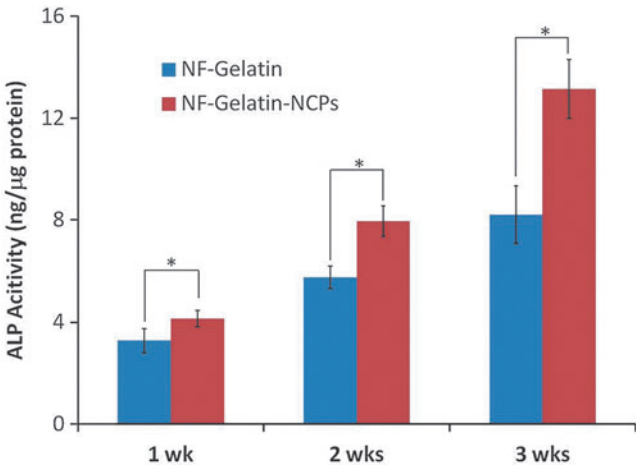

FIG. 4. Alkaline phosphatase (ALP) activity of the MC3T3-E1 osteoblasts cultured on NF-Gelatin and NF-Gelatin-NCPs scaffolds for 3 weeks (*$p < 005$). Color images available online at www.liebertpub.com/tea

indicating that the cells on the NF-Gelatin-NCPs had a higher proliferation rate than on the NF-Gelatin scaffold. The ALP activity increased in both groups from 1 to 3 weeks (Fig. 4). At each time point, the NF-Gelatin-NCPs group always showed significantly higher ALP levels compared to the NF-Gelatin group. The expression of the genes (*OPN, BSP, DMP1, CON,* and *Runx2*) associated with the osteoblastic differentiation was examined using real-time PCR on both the NF-Gelatin-NCPs and NF-Gelatin at 3 weeks. Repeated experiments showed that the expression levels of all these genes were significantly higher in the NF-Gelatin-NCPs than in the NF-Gelatin, indicating that the incorporation of the NCPs onto the surfaces of the NF-Gelatin enhanced the differentiation of the MC3T3-E1 osteoblasts (Fig. 5).

After 3 weeks of cell culture, von Kossa staining revealed a higher amount of mineral deposition in the NF-Gelatin-NCP group than in the NF-Gelatin group (Fig. 6). A high-magnification image showed that the calcium deposition layer on the NF-Gelatin-NCPs was thicker than on the NF-Gelatin group (Fig. 6c, d). Backscattered SEM and μ-CT analysis confirmed these results (Figs. 7 and 8). Furthermore, the μ-CT images indicated that the calcium was deposited evenly throughout the entire NF-Gelatin-NCP scaffold, while the biomineralization was mainly limited to the periphery of the NF-Gelatin scaffold (Fig. 8). Quantitative analysis showed that a significantly higher amount of calcium was deposited on the NF-Gelatin-NCPs (68.4 ± 2.1 μg/scaffold) than on the NF-Gelatin (49.5 ± 3.7 μg/scaffold) (Fig. 9).

In vivo *study*

After 6 weeks' implantation, the scaffolds (NF-Gelatin-NCPs and NF-Gelatin) were retrieved from the rat skull, and μ-CT, histological, and immunohistochemical evaluations

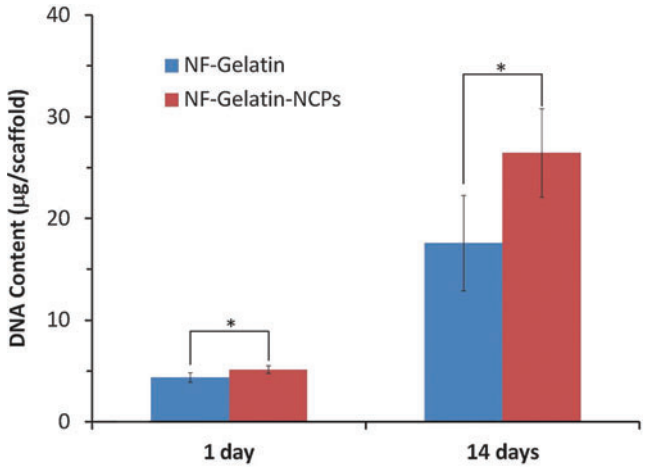

FIG. 3. Proliferation of MC3T3-E1 osteoblasts cultured on NF-Gelatin and NF-Gelatin-NCPs scaffolds for 14 days. About 5×10^5 cells were seeded on each scaffold (*$p < 005$). Color images available online at www.liebertpub.com/tea

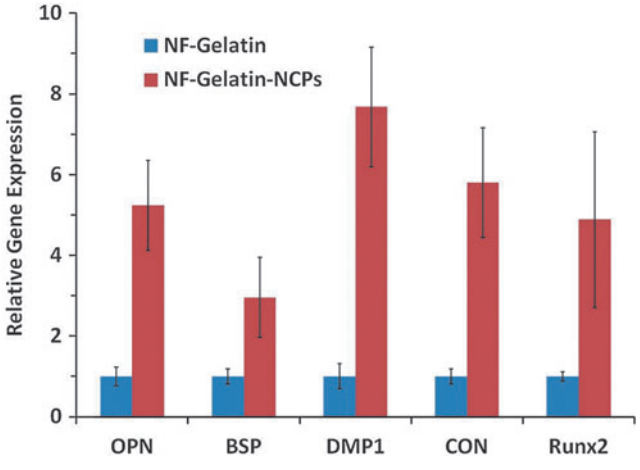

FIG. 5. Relative gene expression (osteopontin [*OPN*], bone sialoprotein [*BSP*], dentin matrix protein 1 [*DMP1*], *CON*, and *Runx2*) after MC3T3-E1 osteoblasts were cultured for 3 weeks on NF-Gelatin and NF-Gelatin-NCPs scaffolds. Color images available online at www.liebertpub.com/tea

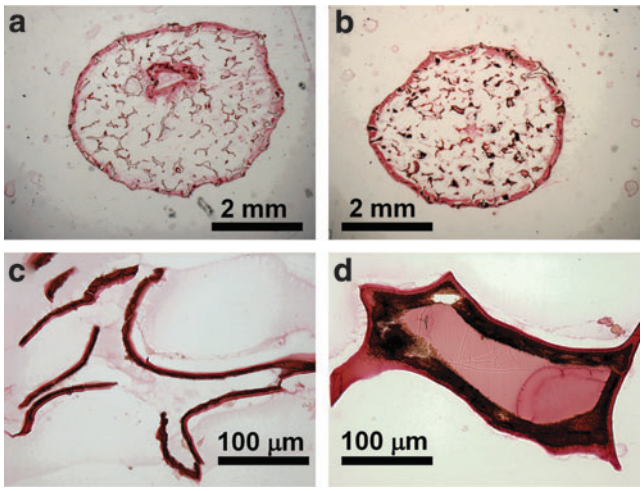

FIG. 6. von Kossa staining of MC3T3-E1 osteoblasts cultured on NF-Gelatin and NF-Gelatin-NCP scaffolds for 3 weeks *in vitro*. **(a)** NF-Gelatin, overview; **(b)** NF-gelatin-NCPs, overview; **(c)** high magnification of **(a)**, showing the mineral deposits on the pore walls of the NF-Gelatin; **(d)** high magnification of **(b)**, showing the mineral deposits on the pore walls of the NF-Gelatin-NCPs. The deposited mineral layer on the NF-Gelatin-NCPs **(d)** is thicker than on the NF-Gelatin **(c)**. Color images available online at www.liebertpub.com/tea

were performed. The μ-CT images showed that there was negligible bone formation in the empty defect (Fig. 10a); a small amount of bone appeared at the native bone margins and the defect periphery on the NF-Gelatin group (Fig. 10b). In contrast, a considerable number of new bones covering most of the defect were observed in the NF-Gelatin-NCP group (Fig. 10c). Quantitative analysis indicated that the amount of bone formation exhibited by the NF-Gelatin-NCPs (BV: $12.16 \pm 1.35\,mm^3$) was 240.6% higher than the NF-Gelatin group (BV: $3.57 \pm 0.83\,mm^3$) (Fig. 10d). The values of the BV/TV in the NF-Gelatin-NCP group ($47.8\% \pm 5.6\%$) were statistically higher than that for the NF-Gelatin group ($12.9 \pm 3.5\%$) (Fig. 10e).

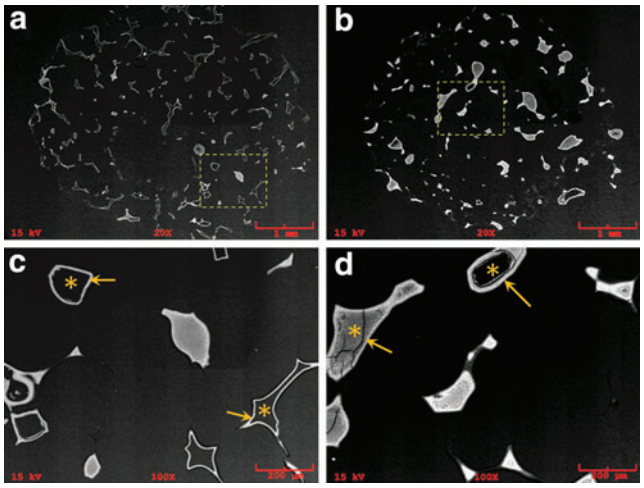

FIG. 7. Backscatter SEM images of MC3T3-E1 osteoblasts cultured on NF-Gelatin and NF-Gelatin-NCP scaffolds for 3 weeks *in vitro*. **(a)** NF-Gelatin, overview; **(b)** NF-gelatin-NCPs, overview; **(c)** higher-magnification view of boxed area in **(a)**; **(d)** higher-magnification view of boxed area in **(b)**. In both **(c)** and **(d)**, * indicates the scaffold and the arrows indicate the deposited minerals from the cells. Color images available online at www.liebertpub.com/tea

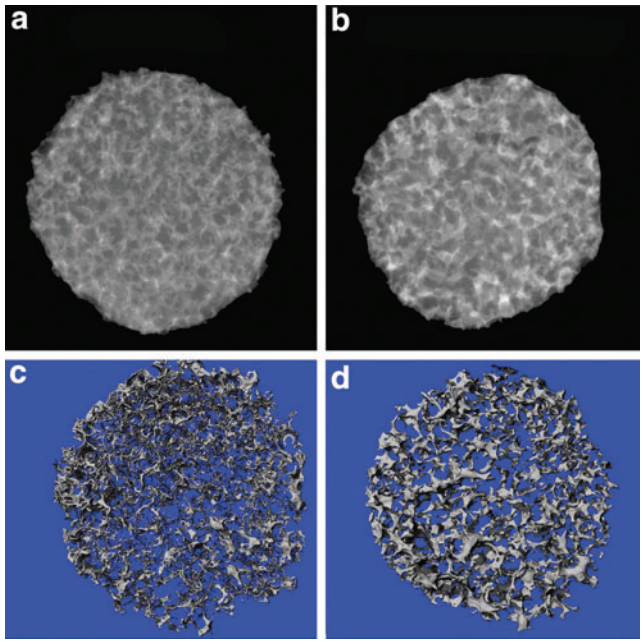

FIG. 8. X-ray and microcomputed tomography (μ-CT) images of MC3T3-E1 osteoblasts cultured on NF-Gelatin and NF-Gelatin-NCP scaffolds for 3 weeks *in vitro*. **(a)** Representative X-ray image of the NF-Gelatin group; **(b)** Representative X-ray image of the NF-Gelatin-NCP group; **(c)** Representative μ-CT image of the NF-Gelatin group; **(d)** Representative μ-CT image of the NF-Gelatin-NCP group. The X-ray and μ-CT images clearly show that more minerals secreted from the osteoblasts were deposited on the NF-Gelatin-NCPs than on the NF-Gelatin, and the deposited minerals were distributed evenly throughout the entire NF-Gelatin-NCPs. Color images available online at www.liebertpub.com/tea

The above findings were further confirmed by histology analyses. As shown in Figure 11a and b, the defect areas of

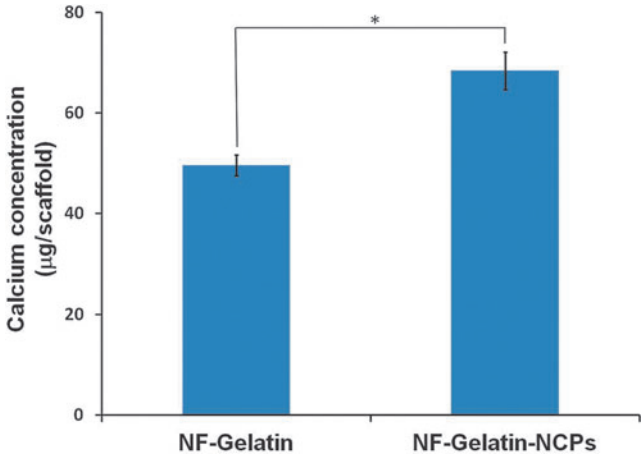

FIG. 9. Calcium content quantification of MC3T3-E1 osteoblasts on NF-Gelatin and NF-Gelatin-NCPs cultured for 3 weeks *in vitro* (*$p < 005$). Color images available online at www.liebertpub.com/tea

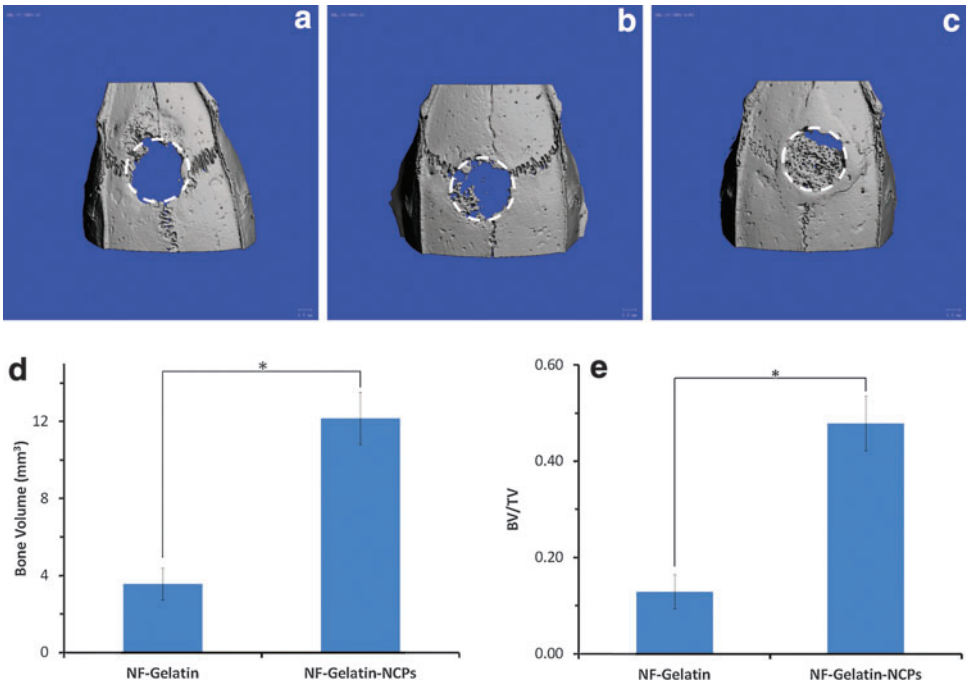

FIG. 10. μ-CT images and quantitative analyses of calvarial bony defects taken 6 weeks after implantation. **(a)** Empty group; **(b)** NF-Gelatin group; **(c)** NF-Gelatin-NCP group. The dotted lines in (a–c) represent the surgical margin of the calvarial defect. **(d)** Bone volumes (BVs) of the NF-Gelatin and NF-Gelatin-NCP constructs after subtracting the value of the negative control (empty group); **(e)** BV to total volume ratio (BV/TV) values of the NF-Gelatin and NF-Gelatin-NCP constructs. The data were expressed as mean ± standard deviation ($n = 4$). *Statistically significant (Student's t-test, $p < 0.05$). Color images available online at www.liebertpub.com/tea

the empty group were entirely filled with fibrous soft tissues. In the NF-Gelatin group, new bone formation was observed, but only on the dura mater side of the calvarial defect (Figs. 11c, d). In comparison, most of the macropores of the NF-Gelatin-NCPs scaffold was filled with newly formed bone tissues (Fig. 11e, f).

To further examine the content of the bone mineralization, immunohistochemistry was performed to determine the expression levels of the mineralization markers (DMP1, BSP, OPN, and OSX). As shown in Figure 12, immunohistochemical staining exhibited a strong expression (dark brown) for DMP1, BSP, OPN, and OSX in the areas of new bone formation within the pore walls of the NF-Gelatin-NCPs samples (as the red arrows indicate in Fig. 12b, d, f), whereas much weaker staining was visible for DMP1, BSP, OPN, and OSX in the NF-Gelatin group. These results confirm that more new bones were regenerated in the NF-Gelatin-NCPs than in the NF-Gelatin scaffold.

Discussion

The ECM of bone is a composite structure whose predominant organic component is type I collagen. The nanofibrous architecture of collagen (type I) in the body has been shown to be important to cellular behavior (adhesion, proliferation, and differentiation),[2,28,29] and a number of technologies have been

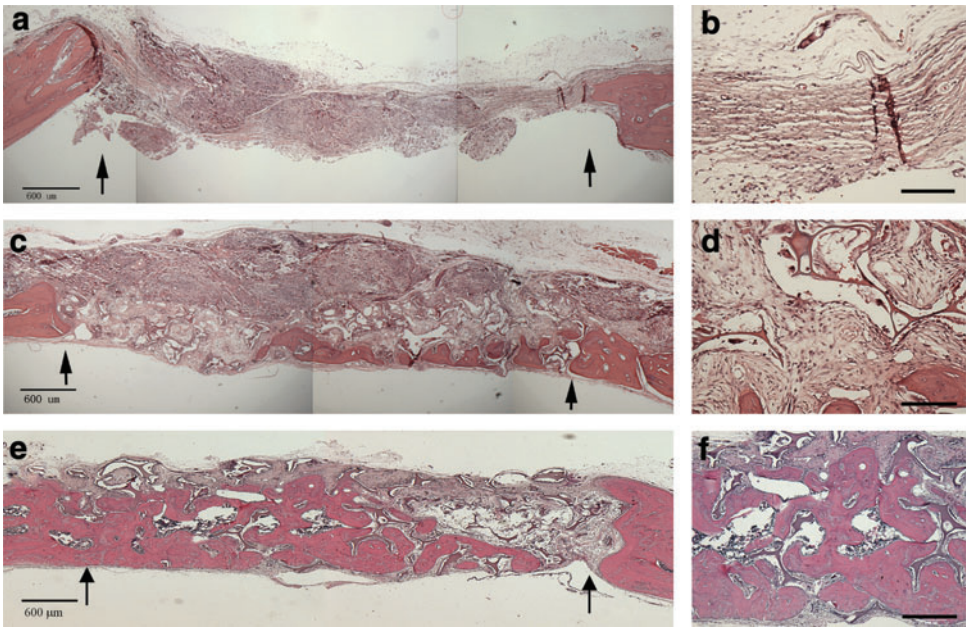

FIG. 11. Histological images of H&E-stained empty group **(a, b)**, NF-Gelatin **(c, d)**, and NF-Gelatin-NCPs **(e, f)** implanted in calvarial defects for 6 weeks. Arrows in **(a, c, e)** mark the surgical margin of original defects. Scale bars in **(a, c, e)** represent 600 μm and in **(b, d, f)** represent 200 μm. Color images available online at www.liebertpub.com/tea

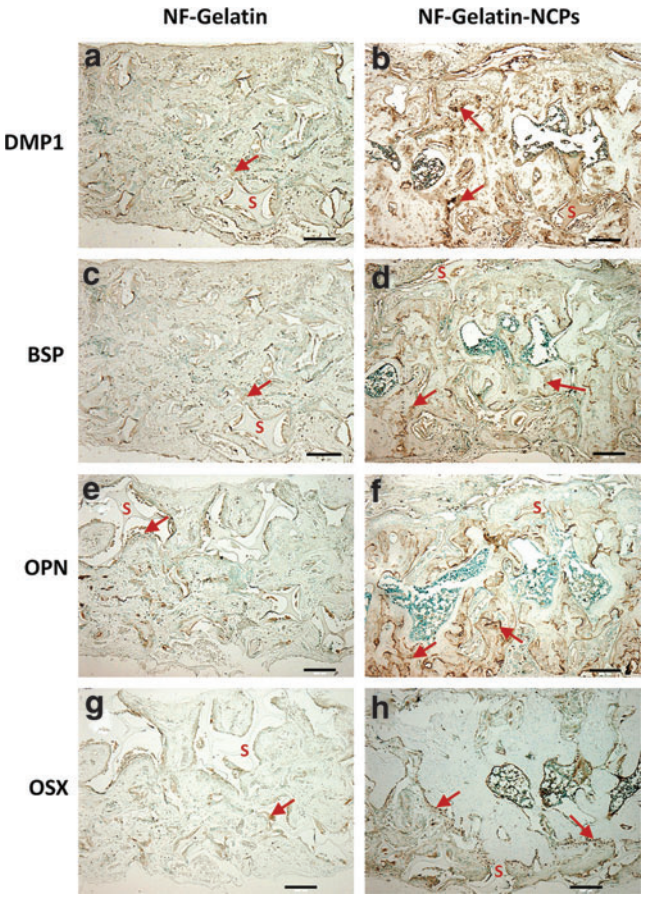

FIG. 12. Immunohistochemical staining for DMP1, BSP, OPN, and OSX in NF-Gelatin **(a, c, e, g)** and NF-Gelatin-NCPs **(b, d, f, h)** implanted in calvarial defects for 6 weeks. In the images, the letter "S" indicates the scaffold and the arrow indicates the stained proteins inside the pore wall of the scaffold. All scale bars represent 200 μm. Color images available online at www.liebertpub.com/tea

reported to mimic its nano-structured architecture,[6,9,10] including the thermally induced phase separation method recently developed in our lab.[6,9,10,16] In addition to type I collagen, there is a variety of other matrix proteins in bone—NCPs, whose effect on bone regeneration has rarely been studied in tissue engineering. In this study, we demonstrated that when the NCPs were integrated with 3D NF-Gelatin scaffolds, these novel biomimetic scaffolds promoted osteoblast proliferation, differentiation, and biomineralization, leading to the regeneration of high-quality bone.

NCPs are bone matrix proteins containing a number of glycoproteins, sialoproteins, and chondroitin sulfate proteoglycans.[19,30–32] For example, one category of NCPs is the small integrin-binding ligand, n-linked glycoprotein (SIBLING) family, which includes BSP, OPN, DSPP, DMP1, and matrix extracellular phosphoglycoprotein.[19] Since these NCPs are acidic and are secreted into the ECM during bone formation and mineralization, they are believed to play key biological roles in initiating and modulating the mineralization of collagen fibers when osteoids are converted into bone.[24] A number of studies have shown that mutation in or knocked out of genes coding for certain NCPs is associated with phenotypic abnormalities in bone mineralization.[22,33–35] However, the way these NPCs in 3D scaffolds affect osteoblast response during bone tissue regeneration is largely unknown. In this work, we developed a surface modification method to couple NCPs with NF-Gelatin scaffolds. Due to the highly interconnected macropores and interstitial spaces between the nanofibers of the scaffold, the NCPs in the reaction solution could easily diffuse into the scaffold and couple with the gelatin molecules on the scaffold surfaces. As the confocal images showed in Figure 1c and d, the NCPs were evenly distributed throughout the entire surfaces (both outer and inner) of 3D gelatin scaffolds. Control of the density of the NCPs on the scaffold surfaces was readily achieved by the NCP concentration during the coupling reaction.

Since the surface-modified biomimetic scaffold mimics both the physical architecture and the chemical compositions of natural bone ECM, we hypothesized that the NF-Gelatin-NCPs would provide a better environment for osteoblast growth and bone tissue formation. As confirmed from the *in vitro* experiments, the number of MC3T3-E1 cells on the NF-Gelatin-NCPs was statistically higher than that on the NF-Gelatin scaffold after culturing for 2 weeks (Fig. 3). Similar to gelatin and other cell adhesion proteins, many NCPs (e.g., BSP, OPN, DMP1, and DSPP) contain the Arg-Gly-Asp (RGD) cell-binding motif.[19,24] In addition, the presence of cryptic cell-binding sites in some NCPs has been reported.[36] Further, recent work has shown that some NCPs (e.g., osteonectin) can enhance cell adhesion to ECM by modulating the conformation of matrix molecules (e.g., collagen) into an active form.[37] We believe that those factors contribute to higher cell numbers on the NF-Gelatin-NCP than on the NC-Gelatin scaffold during the cell culture period. The effects of NCPs on cellular differentiation and biomineralization have been extensively recognized.[36] Among them, BSP is capable of binding collagen type I and nucleating hydroxyl apatite (HA) and, therefore, enhance osteoblast differentiation and biomineralization. DMP1 is needed for normal bone formation, and lack of DMP1 leads to immature osteoblasts in a mutant mouse model.[22] In addition, DMP1 regulate crystal size of the bone mineral.[38] In our study, we found NCPs obviously enhanced the differentiation of MC3T3-E1 seeded on the NF-Gelatin-NCPs. After 3 weeks of culture, the ALP activity and the expression of osteogenic genes (*OPN, BSP, DMP1, CON,* and *Runx2*) on the NF-Gelatin-NCPs were significantly higher than the NF-Gelatin, respectively (Figs. 4 and 5). Our results show that the incorporation of NCPs onto the 3D biomimetic scaffolds significantly enhanced osteoblasts differentiation and mineralization.

Bone mineralization involves the nucleation and growth of HA crystals within the collagenous matrix. Since NCPs bind Ca^{2+} and PO_4^{3-} and have a high affinity for HA, they are postulated to act as both nucleators of HA crystal formation as well as regulators of crystal growth.[25,39] An *in vitro* cell culture study showed that OPN and BSP are two major osteoblast-derived bone proteins that bind to the bone mineral.[39] Our study indicated that adding NCPs into the scaffold increased the thickness of the mineral deposition layer on the surface of the NF-Gelatin-NCPs (Figs. 7 and 8). The calvarial defect implantation experiment also showed better bone tissue formation in the NF-Gelatin-NCPs than in the controls (Figs. 10 and 11). Because no cells were added during implantation, the cells that occupied the NF-Gelatin-NCPs were most likely derived from tissues surrounding the defects: the

periosteum, the dura mater, and the bone tissues. These three types of tissues have been reported to contain stem/progenitor cells for bone formation.[40] A significantly higher amount of bone formed in the NF-Gelatin-NCPs than in the controls after *in vivo* implantation for 6 weeks, which indicates that the NCPs facilitate the recruitment of host cells for tissue regeneration. The exact mechanism of the cell homing process is unknown and warrants further investigation in future studies. Immunohistochemical staining further confirmed a high level of mineralization of bone matrix in the NF-Gelatin-NCPs. Since the NF-Gelatin-NCPs include the NCPs coupling on the surfaces of the scaffold, a weak staining of the proteins (DMP1, BSP, OPN, and OSX) was present on the periphery of the scaffolding pore wall. However, much stronger staining of these proteins was shown inside the pore walls of the scaffold, indicating that the cells from the host were recruited to the NF-Gelatin-NCPs, synthesizing ECM and forming mineralized bone. Taken together, both the *in vitro* and *in vivo* data confirmed that the incorporation of NCPs onto NF-Gelatin scaffolds significantly enhanced osteogenesis and mineralization.

It should be noted that the NCPs extracted from the bone ECM are a mixture and may contain a certain level of key growth factors such as bone morphogenetic protein 2 (BMP2) and fibroblast growth factor (FGF). However, our western blot analyses using specific antibodies for BMP2 and FGF could not identify their presence (data not shown). We believe that the concentration of these molecules in the NCPs is too low to be detected by western blot. Therefore, it is unlikely that these growth factors made a significant contribution to the bone regeneration in our experiments. Instead, other highly expressed acidic matrix proteins (e.g., SIBLING proteins) and proteoglycans are more likely to play a major role during the process of osteogenesis and mineralization. It is not clear which component of the bone NCPs plays dominant roles in the regeneration of bone in this work. Future studies will focus on the dissection of the effects of a single protein in the NCPs on bone regeneration.

Conclusions

NCPs were extracted from bone ECM and successfully coupled to the surfaces of NF-Gelatin scaffolds. The *in vitro* results showed that the NF-Gelatin-NCPs promoted osteoblast proliferation, differentiation, and mineralization. The *in vivo* calvarial defect study indicated that the NF-Gelatin-NCPs recruited more host cells to the defect and regenerated a higher amount of bone than did the controls after 6-week implantation. The integration of NCPs into NF-gelatin scaffolds, therefore, is a promising strategy for improving bone regeneration.

Acknowledgments

This work was supported by Research Grant NIH/NIDCR-DE020742 to R.D.S., NIH/NIDCR-DE005092 to C.Q., and Texas A&M-Weizmann Collaborative Program to X.L. We would like to thank Jeanne Santa Cruz for assistance with editing of this article.

Disclosure Statement

No competing financial interests exist.

References

1. Shin, H., Jo, S., and Mikos, A.G. Biomimetic materials for tissue engineering. Biomaterials **24,** 4353, 2003.
2. Ma, P.X. Biomimetic materials for tissue engineering. Adv Drug Deliv Rev **60,** 184, 2008.
3. Liu, X.H., and Ma, P.X. Polymeric scaffolds for bone tissue engineering. Ann Biomed Eng **32,** 477, 2004.
4. Ruiz-Hitzky, E., Darder, M., Aranda, P., and Ariga, K. Advances in biomimetic and nanostructured biohybrid materials. Adv Mater **22,** 323, 2010.
5. Huebsch, N., and Mooney, D.J. Inspiration and application in the evolution of biomaterials. Nature **462,** 426, 2009.
6. Li, W.J., Laurencin, C.T., Caterson, E.J., Tuan, R.S., and Ko, F.K. Electrospun nanofibrous structure: a novel scaffold for tissue engineering. J Biomed Mater Res **60,** 613, 2002.
7. Li, M., Mondrinos, M., Gandhi, M., Ko, F., Weiss, A., and Lelkes, P. Electrospun protein fibers as matrices for tissue engineering. Biomaterials **26,** 5999, 2005.
8. Pham, Q.P., Sharma, U., and Mikos, A.G. Electrospinning of polymeric nanofibers for tissue engineering applications: a review. Tissue Eng **12,** 1197, 2006.
9. Zhang, S.G. Fabrication of novel biomaterials through molecular self-assembly. Nat Biotechnol **21,** 1171, 2003.
10. Hartgerink, J.D., Beniash, E., and Stupp, S.I. Self-assembly and mineralization of peptide-amphiphile nanofibers. Science **294,** 1684, 2001.
11. Karageorgiou, V., and Kaplan, D. Porosity of 3D biornaterial scaffolds and osteogenesis. Biomaterials **26,** 5474, 2005.
12. Greiner, A., and Wendorff, J.H. Electrospinning: a fascinating method for the preparation of ultrathin fibres. Angew Chem Int Edit **46,** 5670, 2007.
13. Cui, H., Webber, M.J., and Stupp, S.I. Self-assembly of peptide amphiphiles: from molecules to nanostructures to biomaterials. Biopolymers **94,** 1, 2010.
14. Gillette, B.M., Jensen, J.A., Tang, B., Yang, G.J., Bazargan-Lari, A., Zhong, M., *et al. In situ* collagen assembly for integrating microfabricated three-dimensional cell-seeded matrices. Nat Mater **7,** 636, 2008.
15. Hartgerink, J.D. Supramolecular chemistry and self-assembly special feature: peptide-amphiphile nanofibers: a versatile scaffold for the preparation of self-assembling materials. Proc Natl Acad Sci U S A **99,** 5133, 2002.
16. Liu, X.H., and Ma, P.X. Phase separation, pore structure, and properties of nanofibrous gelatin scaffolds. Biomaterials **30,** 4094, 2009.
17. Liu, X., Smith, L.A., Hu, J., and Ma, P.X. Biomimetic nanofibrous gelatin/apatite composite scaffolds for bone tissue engineering. Biomaterials **30,** 2252, 2009.
18. Butler, W.T., and Ritchie, H. The nature and functional-significance of dentin extracellular matrix proteins. Int J Dev Biol **39,** 169, 1995.
19. Qin, C., Baba, O., and Butler, W.T. Post-translational modifications of sibling proteins and their roles in osteogenesis and dentinogenesis. Crit Rev Oral Biol Med **15,** 126, 2004.
20. Bellahcene, A., Castronovo, V., Ogbureke, K.U.E., Fisher, L.W., and Fedarko, N.S. Small integrin-binding ligand N-linked glycoproteins (SIBLINGs): multifunctional proteins in cancer. Nat Rev Cancer **8,** 212, 2008.
21. Almushayt, A., Narayanan, K., Zaki, A.E., and George, A. Dentin matrix protein 1 induces cytodifferentiation of dental pulp stem cells into odontoblasts. Gene Ther **13,** 611, 2006.
22. Feng, J.Q., Ward, L.M., Liu, S.G., Lu, Y.B., Xie, Y.X., Yuan, B.Z., *et al.* Loss of DMP1 causes rickets and osteomalacia and

identifies a role for osteocytes in mineral metabolism. Nat Genet **38,** 1310, 2006.
23. Prescott, R.S., Alsanea, R., Tayad, M.I., Johnson, B.R., Wenckus, C.S., Hao, J., *et al. In vivo* generation of dental pulp-like tissue by using dental pulp stem cells, dentin matrix protein 1 transplantation in mice. J Endodont **34,** 421, 2008.
24. Huang, B.Z., Sun, Y., Maciejewska, I., Qin, D.S., Peng, T., McIntyre, B., *et al.* Distribution of SIBLING proteins in the organic and inorganic phases of rat dentin and bone. Eur J Oral Sci **116,** 104, 2008.
25. Boskey, A.L. Noncollagenous matrix proteins and their role in mineralization. Bone Miner **6,** 111, 1989.
26. Lu, Y.B., Yuan, B.Z., Qin, C.L., Cao, Z.G., Xie, Y.X., Dallas, S.L., *et al.* The biological function of DMP-1 in osteocyte maturation is mediated by its 57-kDa C-terminal fragment. J Bone Miner Res **26,** 331, 2011.
27. Baba, O., Qin, C.L., Brunn, J.C., Wygant, J.N., McIntyre, B.W., and Butler, W.T. Colocalization of dentin matrix protein 1 and dentin sialoprotein at late stages of rat molar development. Matrix Biol **23,** 371, 2004.
28. Kleinman, H.K., Klebe, R.J., and Martin, G.R. Role of collagenous matrices in the adhesion and growth of cells. J Cell Biol **88,** 473, 1981.
29. Lee, C.H., Singla, A., and Lee, Y. Biomedical applications of collagen. Int J Pharm **221,** 1, 2001.
30. Gorski, J.P. Is all bone the same? Distinctive distributions and properties of non-collagenous matrix proteins in lamellar vs. woven bone imply the existence of different underlying osteogenic mechanisms. Crit Rev Oral Biol Med **9,** 201, 1998.
31. Qin, C.L., Brunn, J.C., Jones, J., George, A., Ramachandran, A., Gorski, J.P., *et al.* A comparative study of sialic acid-rich proteins in rat bone and dentin. Eur J Oral Sci **109,** 133, 2001.
32. Termine, J.D., Belcourt, A.B., Conn, K.M., and Kleinman, H.K. Mineral and collagen-binding proteins of fetal calf bone. J Biol Chem **256,** 403, 1981.
33. Xiao, S.X., Yu, C., Chou, X.M., Yuan, W.J., Wang, Y., Bu, L., *et al.* Dentinogenesis imperfecta 1 with or without progressive hearing loss is associated with distinct mutations in DSPP. Nat Genet **27,** 201, 2001.
34. Sreenath, T., Thyagarajan, T., Hall, B., Longenecker, G., D'Souza, R., Hong, S., *et al.* Dentin sialophosphoprotein knockout mouse teeth display widened predentin zone and develop defective dentin mineralization similar to human dentinogenesis imperfecta type III. J Biol Chem **278,** 24874, 2003.
35. Rittling, S.R., Matsumoto, H.N., McKee, M.D., Nanci, A., An, X.R., Novick, K.E., *et al.* Mice lacking osteopontin show normal development and bone structure but display altered osteoclast formation *in vitro*. J Bone Miner Res **13,** 1101, 1998.
36. Alford, A.I., and Hankenson, K.D. Matricellular proteins: extracellular modulators of bone development, remodeling, and regeneration. Bone **38,** 749, 2006.
37. Koblinski, J.E., Wu, M., Demeler, B., Jacob, K., and Kleinman, H.K. Matrix cell adhesion activation by non-adhesion proteins. J Cell Sci **118,** 2965, 2005.
38. Tartaix, P.H., Doulaverakis, M., George, A., Fisher, L.W., Butler, W.T., Qin, C.L., *et al. In vitro* effects of dentin matrix protein-1 on hydroxyapatite formation provide insights into *in vivo* functions. J Biol Chem **279,** 18115, 2004.
39. Nagata, T., Bellows, C.G., Kasugai, S., Butler, W.T., and Sodek, J. Biosynthesis of bone proteins SPP-1,BSP and SPARC in association with mineralized tissue formation by fetal rat calvarial cells in culture. Biochem J **274,** 513, 1991.
40. Gosain, A.K., Santoro, T.D., Song, L.S., Capel, C.C., Sudhakar, P.V., and Madoub, H.S. Osteogenesis in calvarial defects: contribution of the dura, the pericranium, and the surrounding bone in adult versus infant animals. Plast Reconstr Surg **112,** 515, 2003.

Address correspondence to:
Xiaohua Liu, PhD
Biomedical Science Department
The Center for Craniofacial Research and Diagnosis
Texas A&M University Baylor College of Dentistry
Dallas, TX 75246

E-mail: xliu@bcd.tamhsc.edu

Received: September 18, 2012
Accepted: March 1, 2013
Online Publication Date: April 4, 2013